

# Chain-Length-Dependent Conformational Transformation and Melting Behavior of Alkyl/Oligo(oxyethylene)/Alkyl Triblock Compounds: $\alpha$ -Hexyl- $\omega$ -hexyloxyoligo(oxyethylene)s

Koichi Fukuhara,\* Takahiro Mizawa, Tomohiro Inoue, Hirotaka Kumamoto, and Hiroatsu Matsuura

Department of Chemistry, Graduate School of Science, Hiroshima University, Kagamiyama, Higashi-Hiroshima 739-8526, Japan

Received: April 29, 2003; In Final Form: August 7, 2003

The chain-length-dependent conformational transformation and melting behavior of triblock compounds  $\alpha$ -hexyl- $\omega$ -hexyloxyoligo(oxyethylene)s,  $\text{H}(\text{CH}_2)_6(\text{OCH}_2\text{CH}_2)_m\text{O}(\text{CH}_2)_6\text{H}$  (abbreviated as  $\text{C}_6\text{E}_m\text{C}_6\text{S}$ ) ( $m = 1-7$ ), have been studied by differential scanning calorimetry and infrared spectroscopy. With an increase in the number of oxyethylene units ( $m$ ), the molecular form of the triblock compounds in the solid state changes from an all-trans planar form ( $\gamma$  form) to a planar/helical/planar triblock form ( $\beta$  form) at  $m = 5$ . The melting points of the  $\gamma$  form  $\text{C}_6\text{E}_m\text{C}_6\text{S}$  are much lower than the melting points of  $n$ -alkanes with similar molecular masses. This result is interpreted as due to the higher Gibbs energy of crystal for  $\text{C}_6\text{E}_m\text{C}_6\text{S}$ . The observed thermodynamic quantities indicate that the planar structure of the oligo(oxyethylene) chain is stabilized by the force of the magnitude that maintains the rotator phase of  $n$ -alkanes. The  $\beta$ -form  $\text{C}_6\text{E}_m\text{C}_6\text{S}$  melt stepwise through a solid–solid transition, at which the melting of only the alkyl blocks of the molecule occurs. The alkyl chains in the  $\beta$ -form  $\text{C}_6\text{E}_m\text{C}_6\text{S}$  are loosely packed in the crystal even below the solid–solid transition temperature, while the crystallinity of the oligo(oxyethylene) block is significantly high. The molecular form of the alkyl/oligo(oxyethylene)/alkyl triblock compounds in the solid state is determined by the balance of the intramolecular conformational restoring force in the central oligo(oxyethylene) block and the intermolecular packing force in the end alkyl blocks. The conformational restoring force results from a tendency of the oligo(oxyethylene) chain to resume its intrinsic helical structure.

## Introduction

The higher order structures formed by block copolymers consisting of component blocks that tend to crystallize have attracted much attention in the field of soft materials science as a new design for mesoscopic structures.<sup>1–4</sup> One of the important factors that govern the formation of mesoscopic structures of crystallizable copolymers is polymorphism of the constituent blocks. Booth and co-workers have studied conformational polymorphism for a series of block compounds consisting of alkyl chains that favor an extended zigzag structure and an oligo(oxyethylene) chain that favors a helical structure.<sup>5,6</sup> Their systematic studies using various experimental methods such as differential scanning calorimetry (DSC), X-ray scattering, and infrared and Raman spectroscopy revealed that there are three types of structures with different crystallinity for alkyl/oligo(oxyethylene)/alkyl triblock compounds  $\text{H}(\text{CH}_2)_n(\text{OCH}_2\text{CH}_2)_m\text{O}(\text{CH}_2)_{n'}\text{H}$  ( $\alpha$ - $n$ -alkyl- $\omega$ - $n'$ -alkoxyoligo(oxyethylene)s, abbreviated as  $\text{C}_n\text{E}_m\text{C}_{n'}$ ) with  $n = 1-26$  and  $m = 9$  and  $15$ . More recently, we have observed chain-length-dependent conformational polymorphism and transformation for a series of  $\text{C}_n\text{E}_m\text{C}_{n'}$  compounds with  $n = 3-10$ ,  $m = 1-8$ , and  $n' = 1-7$  using infrared and Raman spectroscopy and have found two distinctive molecular forms in the solid state, namely a highly extended all-trans planar form ( $\gamma$  form) and a planar/helical/planar triblock form ( $\beta$  form).<sup>7–12</sup> These molecular forms are depicted in Figure 1.

The all-trans planar form of the  $\text{C}_n\text{E}_m\text{C}_{n'}$  compounds, called the  $\gamma$  form, has been found for the homologues with the end

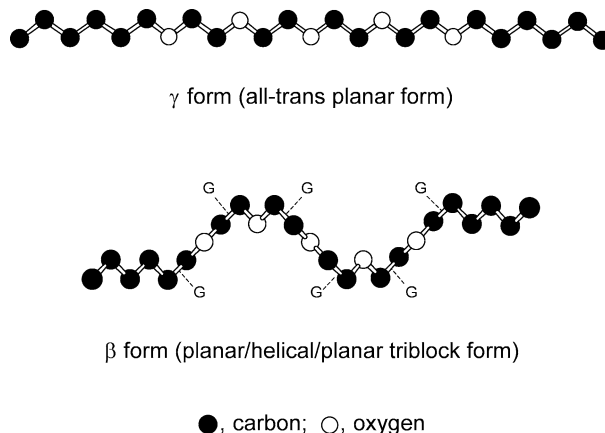


**Figure 1.** Skeletal models of the  $\text{C}_n\text{E}_m\text{C}_{n'}$  molecule. The models of  $\text{C}_6\text{E}_4\text{C}_6$  are shown as an illustration. Only the bonds in the gauche conformation are indicated by G; others are in the trans conformation.

alkyl blocks with their total length (the total number of backbone atoms) longer than the length of the central oligo(oxyethylene) block.<sup>9,12</sup> For this form, the oligo(oxyethylene) chain, which intrinsically prefers to assume a helical structure with a repeated trans–gauche–trans conformation for the  $\text{O}-\text{CH}_2-\text{CH}_2-\text{O}$  group in the solid state,<sup>13</sup> assumes alternatively a planar structure with the all-trans conformation. The planar/helical/planar triblock form, on the other hand, has been observed for the homologues with the end alkyl blocks with their total length shorter than the length of the central oligo(oxyethylene) block. For this triblock form, two conformational types have been found, the  $\beta$  form and the  $\alpha\beta$  form.<sup>7,9,12</sup> The difference between

\* To whom correspondence should be addressed. E-mail: kfuku@sci.hiroshima-u.ac.jp.

these forms lies in the conformation around the CC–CO bonds adjoining the central oligo(oxyethylene) block; the  $\beta$  form assumes the gauche conformation around two of these bonds in the molecule, while the  $\alpha\beta$  form assumes the gauche conformation around one of these and the trans conformation around the other. The chain-length-dependent conformational transformation from the  $\gamma$  form into the  $\beta$  (or  $\alpha\beta$ ) form or the transformation vice versa has been attributed to a crystallization competition between the oligo(oxyethylene) and alkyl blocks.<sup>12</sup> If the crystallization of the alkyl blocks takes place faster than the crystallization of the oligo(oxyethylene) block, the void for the oligo(oxyethylene) chain to fit in, allowed by the planar structure of the alkyl blocks, is too small provided the oligo(oxyethylene) chain crystallizes with a helical structure. The oligo(oxyethylene) chain then crystallizes by assuming an alternative planar structure.

In light of the results so far obtained, we direct our attention to a relation between the chain-length-dependent conformational transformation and melting behavior of the  $C_nE_mC_n$  triblock compounds; the subjects to be studied are (1) the balance of intramolecular and intermolecular forces acting in the solid state and (2) the melting behavior of the  $\gamma$  form triblock compounds in comparison with the melting behavior of  $n$ -alkanes. With respect to subject (1), the forces concerned include an intramolecular conformational restoring force in the oligo(oxyethylene) block, an intermolecular cohesive force in the alkyl blocks due to van der Waals force, and an intermolecular force due to local dipole–dipole interactions of the polar C–O bonds. The conformational restoring force in the oligo(oxyethylene) block results from a tendency of the oligo(oxyethylene) chain to resume the helical structure. Namely, the planar oligo(oxyethylene) chain has a propensity to revert to its intrinsic helical structure.<sup>14</sup> Thus, for the all-trans planar  $\gamma$  form, the intramolecular conformational restoring force in the oligo(oxyethylene) block opposes the intermolecular cohesive force in the alkyl blocks. Another intermolecular force, the local dipole–dipole interaction of the C–O bonds, is a possible force affecting the stability of  $C_nE_mC_n$  crystals. This force is attractive or repulsive depending on the orientation of the relevant bonds.

In subject (2), the comparison of the melting behavior of the  $\gamma$  form  $C_nE_mC_n$ s with that of  $n$ -alkanes is of great interest from structural and thermodynamical points of view, because the molecular geometry of the  $\gamma$  form is similar to that of  $n$ -alkanes in the solid state. Recently, we have studied the melting behavior of the  $\gamma$  form symmetric  $C_nE_mC_n$  triblock compounds and obtained several interesting results including significantly lower melting points of  $C_nE_mC_n$ s than those of the corresponding  $n$ -alkanes and a relation between the conformational stability and thermal behavior of  $C_nE_mC_n$ s.<sup>15</sup>

In this work, we studied the conformational transformation and melting behavior of a series of  $C_6E_mC_6$  compounds to elucidate subjects (1) and (2) described above. The purity of the samples used in the previous work was 95–99%, which was not high enough to perform accurate thermal analysis. Accordingly, we have further purified the relevant  $C_6E_mC_6$  samples ( $m = 1–7$ ) to be better than 99.7%. Using the purified samples, we performed precise measurements of DSC and infrared spectroscopy.

## Experimental Section

**Materials.** The  $C_6E_mC_6$  compounds with  $m = 1–4$  were prepared from 1-chlorohexane and mono-, di-, tri-, and tetraethylene glycols, respectively, with tetrabutylammonium hydrogensulfate as a phase transfer catalyst.<sup>16</sup> The  $C_6E_mC_6$

compounds with  $m = 5–7$  were prepared with use of the same catalyst from 1-chloro-3,6-dioxadodecane and mono-, di-, and triethylene glycols, respectively. All products were purified by repeated vacuum distillations and Kugelrohr distillation. Some of the  $C_6E_mC_6$ s were purified by column chromatography on silica gel prior to the distillation. The purity was checked by gas chromatography to be 99.8% for  $C_6E_1C_6$ , 99.9% for  $C_6E_2C_6$ , 99.9% for  $C_6E_3C_6$ , 99.9% for  $C_6E_4C_6$ , 99.7% for  $C_6E_5C_6$ , 99.9% for  $C_6E_6C_6$ , and 99.8% for  $C_6E_7C_6$ .

**DSC Measurements.** The DSC melting curves of  $C_6E_mC_6$ s ( $m = 1–7$ ) were measured on a Shimadzu DSC-50 differential scanning calorimeter equipped with a Shimadzu LTC-50 cooling jacket. The thermodynamic quantities, i.e., melting point, solid–solid transition temperature, enthalpy of melting, and enthalpy of solid–solid transition, were measured over a temperature range from 230 to 290 K. A rate of heating of 3.0 deg min<sup>−1</sup> was adopted as standard in this work. Measurements with different rates of heating, i.e., 0.1, 0.3, 1.0, and 10.0 deg min<sup>−1</sup>, were also performed to examine possible effect of the scan rate on DSC curves. Before the measurements, the solidified samples were kept at about 220 K for 30 min. Annealing was also applied to the solidified samples to examine the thermal history dependency of the DSC curves. The temperature and the enthalpy change were calibrated by using the standard samples,  $n$ -dodecane and indium. The reproducibility of the observed DSC melting curves was confirmed by the measurements on different samples of the same compound.

**Infrared Measurements.** The infrared spectra of  $C_6E_mC_6$ s were recorded on a Perkin-Elmer Spectrum One Fourier transform spectrometer with a spectral resolution of 2.0 cm<sup>−1</sup>. The spectrometer was purged with dry nitrogen gas before the measurements. A Peltier cryostat cell was used to measure the infrared spectra in a temperature range from 230 to 290 K.

## Results and Discussion

**Overview of Melting Behavior of  $C_6E_mC_6$ s.** It was shown in the present DSC experiments that the signals are not dependent on the rate of heating in a 0.1–10.0 deg min<sup>−1</sup> range, except for the case of  $C_6E_5C_6$  (unannealed) as will be described later. The DSC melting curves of  $C_6E_mC_6$ s ( $m = 1–7$ ) measured at a rate of heating 3.0 deg min<sup>−1</sup> are shown in Figure 2. The observed curves are classified into two types according to their appearance, one that exhibits a single endothermic peak, observed by  $C_6E_1C_6$  though  $C_6E_4C_6$  and  $C_6E_5C_6$  (annealed), and the other that exhibits two main endothermic peaks, observed by  $C_6E_3C_6$  (unannealed),  $C_6E_6C_6$ , and  $C_6E_7C_6$ . The alteration of the type of DSC curves for  $C_6E_mC_6$ s at  $m = 5$  should reflect the change of molecular conformation at this length of the oligo(oxyethylene) block. It is noted that  $C_6E_5C_6$  gave two different DSC melting curves, one for the unannealed sample solidified from the liquid and the other for the sample annealed at about 260 K for more than 1 h. This thermal history dependency suggests that  $C_6E_5C_6$  has a propensity for polymorphism.

A closer examination indicates that, for  $C_6E_4C_6$  and  $C_6E_5C_6$  (annealed), a weak unresolved shoulder is observed at the lower temperature side of the main peak. Although this shoulder is most probably assigned to a solid–solid transition, we consider the apparent composite peak for these compounds as a single endothermic peak associated with the melting, as we could not separate the shoulder from the main peak even at a slower 0.1 deg min<sup>−1</sup> rate of heating. The observation of two main endothermic peaks as well as ill-defined peak(s) for  $C_6E_3C_6$  (unannealed),  $C_6E_6C_6$ , and  $C_6E_7C_6$  suggests a stepwise melting process. We will consider only the two main endotherms

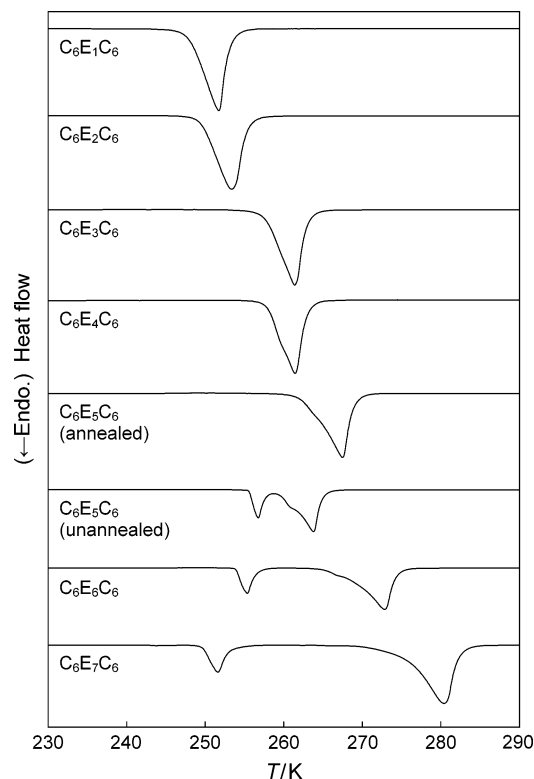


Figure 2. DSC melting curves of  $C_6E_mC_6s$  ( $m = 1-7$ ).

associated with a solid–solid transition and the melting in subsequent discussion.

**Polymorphism of  $C_6E_5C_6$ .** As described above,  $C_6E_5C_6$  gives, depending on whether the sample is annealed or unannealed, two different DSC curves when heated at a rate of  $3.0 \text{ deg min}^{-1}$  (Figure 2). It was also found that the contour of the DSC curve for  $C_6E_5C_6$  (unannealed) changes with varying rate of heating in a range below  $1.0 \text{ deg min}^{-1}$ . This observation suggests that a slow transition takes place from the unannealed solid to the annealed solid during these DSC measurements. According to our previous Raman spectroscopic study,<sup>9</sup>  $C_6E_5C_6$  gave a single type of spectrum ( $\beta$  form) irrespective of the thermal treatment. To be consistent with the present DSC observation, this compound is anticipated to give two types of spectra depending on the thermal treatment. Using the sample of higher purity, we have reexamined the infrared spectra of  $C_6E_5C_6$  in the solid state and actually found two different spectra.

Figure 3 shows the infrared spectra of  $C_6E_5C_6$ , annealed and unannealed, at 235 K, along with the spectra of  $C_6E_4C_6$  ( $\gamma$  form) and  $C_6E_6C_6$  ( $\beta$  form) as comparison. The spectrum of annealed  $C_6E_5C_6$  has common features to the spectrum of  $C_6E_4C_6$ ; a distinct band at  $1495\text{--}1500 \text{ cm}^{-1}$  and a strong band at  $960\text{--}965 \text{ cm}^{-1}$  are characteristic of the all-trans planar  $\gamma$  form.<sup>12</sup> These features evidence that the molecular form of annealed  $C_6E_5C_6$  is the  $\gamma$  form. The spectrum of unannealed  $C_6E_5C_6$ , on the other hand, shows the features that have been observed for  $C_6E_6C_6$ . A well-defined band at about  $1280 \text{ cm}^{-1}$ , strong bands centered around  $1110 \text{ cm}^{-1}$ , and a complex spectral feature in the  $800\text{--}900\text{-cm}^{-1}$  region are assigned to the trans–gauche–trans conformation of the  $\text{CH}_2\text{O--CH}_2\text{--CH}_2\text{--OCH}_2$  group in the oligo(oxyethylene) chain.<sup>17</sup> The weak bands at 723, 748, and  $817 \text{ cm}^{-1}$ , which are the spectral features common to  $C_6E_5C_6$  (unannealed) and  $C_6E_6C_6$ , are assigned to the  $\text{CH}_3\text{CH}_2\text{--CH}_2\text{--CH}_2\text{--CH}_2\text{--CH}_2\text{O}$  group in the (trans)<sub>3</sub>–gauche conformation.<sup>12</sup> These observations indicate that the molecular form

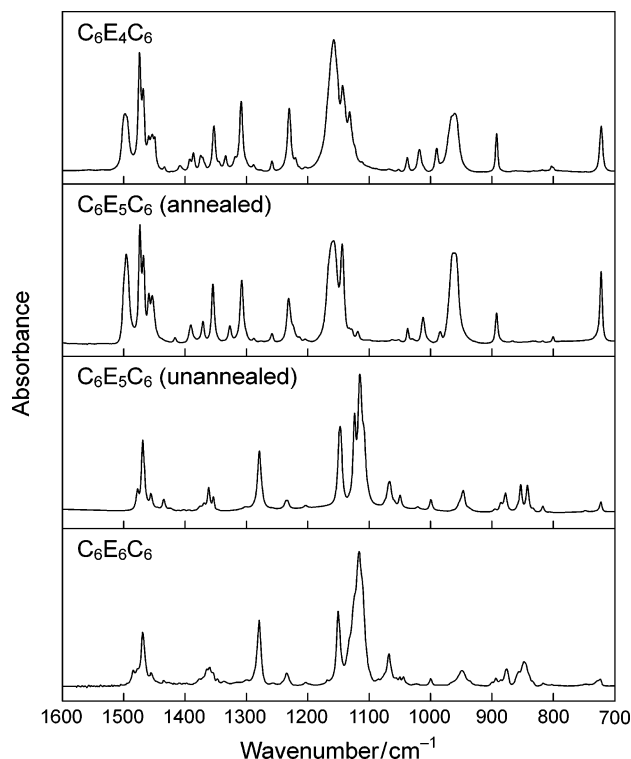


Figure 3. Infrared spectra of  $C_6E_mC_6$  ( $m = 4-6$ ) at 235 K.

TABLE 1. Molecular Forms<sup>a</sup> of  $C_6E_mC_6s$  ( $m = 1-7$ ) in the Solid State

$m = 1$	$m = 2$	$m = 3$	$m = 4$	$m = 5$		$m = 6$	$m = 7$
				annealed	unannealed		
$\gamma$	$\gamma$	$\gamma$	$\gamma$	$\gamma$	$\beta$	$\beta$	$\beta$

<sup>a</sup> For the molecular forms, see Figure 1.

of unannealed  $C_6E_5C_6$  is the  $\beta$  form. The  $\gamma$  form for the annealed solid is a stable form of  $C_6E_5C_6$ , and the polymorphism of the molecule, being of the  $\gamma$  form or the  $\beta$  form, is monotropic, because an exothermic peak (the data not shown) was observed at the transition from the  $\beta$  form to the  $\gamma$  form in the process of annealing. The molecular forms of  $C_6E_mC_6s$  ( $m = 1-7$ ) in the solid state are summarized in Table 1. It is shown for this series of homologues that the molecular form transforms from the all-trans planar  $\gamma$  form to the planar/helical/planar triblock  $\beta$  form at  $m = 5$ .

**Melting Behavior of  $C_6E_mC_6s$ .** The thermodynamic quantities of  $C_6E_mC_6s$  ( $m = 1-7$ ) derived from the DSC melting curves measured at a rate of heating of  $3.0 \text{ deg min}^{-1}$  are listed in Table 2, where the transition temperature is taken at an extrapolated onset of the relevant DSC peak and the entropy of melting (or transition) is given as the enthalpy of melting (transition) divided by the melting point (transition temperature). The dependencies of the melting point ( $T_m$ ) and the solid–solid transition temperature ( $T_t$ ) on relative molecular mass ( $M_r$ ) are shown in Figure 4. The corresponding dependencies for  $n$ -alkanes of the melting point of the rotator phase ( $T_{m(ro)}$ ) and the crystalline–rotator phase transition temperature ( $T_{t(cry-ro)}$ )<sup>18–20</sup> are also given in the same figure for comparison.<sup>21</sup> In Figure 4 and the subsequent two figures, the data points for  $C_6E_mC_6s$  at  $m = 1-5$ , connected by straight lines, are those of the  $\gamma$  form, and the data points at  $m = 5-7$  are of the  $\beta$  form.

Figure 5 shows the dependencies on  $M_r$  of the enthalpy of melting ( $\Delta H_m$ ) and the enthalpy of solid–solid transition ( $\Delta H_t$ ) for  $C_6E_mC_6s$ , along with those of the enthalpy of melting of the

TABLE 2. Thermodynamic Quantities<sup>a</sup> of C<sub>6</sub>E<sub>m</sub>C<sub>6</sub>s (*m* = 1–7)

compd	<i>T<sub>m</sub></i> <sup>b</sup> /K	Δ <i>H<sub>m</sub></i> /kJ mol <sup>−1</sup>	Δ <i>S<sub>m</sub></i> <sup>c</sup> /J K <sup>−1</sup> mol <sup>−1</sup>	<i>T<sub>t</sub></i> <sup>b</sup> /K	Δ <i>H<sub>t</sub></i> /kJ mol <sup>−1</sup>	Δ <i>S<sub>t</sub></i> <sup>d</sup> /J K <sup>−1</sup> mol <sup>−1</sup>
γ form (all-trans planar form)						
C <sub>6</sub> E <sub>1</sub> C <sub>6</sub>	248.2	41.47(0.14)	167.1(0.6)			
C <sub>6</sub> E <sub>2</sub> C <sub>6</sub>	249.5	46.46(0.10)	186.2(0.4)			
C <sub>6</sub> E <sub>3</sub> C <sub>6</sub>	257.5	53.82(0.18)	209.0(0.7)			
C <sub>6</sub> E <sub>4</sub> C <sub>6</sub>	258.0	59.31(0.16)	229.9(0.6)			
C <sub>6</sub> E <sub>5</sub> C <sub>6</sub> (annealed)	263.0(0.1)	66.31(0.01)	252.1(0.1)			
β form (planar/helical/planar triblock form)						
C <sub>6</sub> E <sub>5</sub> C <sub>6</sub> (unannealed)	260.3(0.1)	47.86(0.51)	183.9(1.8)	255.4(0.1)	13.91(0.05)	54.5(0.2)
C <sub>6</sub> E <sub>6</sub> C <sub>6</sub>	268.3	55.97(0.49)	208.6(1.9)	254.0	13.61(0.02)	53.6(0.1)
C <sub>6</sub> E <sub>7</sub> C <sub>6</sub>	276.2	64.46(0.11)	233.4(0.4)	251.5	14.00(0.14)	55.7(0.6)

<sup>a</sup> *T<sub>m</sub>*, melting point; Δ*H<sub>m</sub>*, enthalpy of melting; Δ*S<sub>m</sub>*, entropy of melting; *T<sub>t</sub>*, solid–solid transition temperature; Δ*H<sub>t</sub>*, enthalpy of solid–solid transition; Δ*S<sub>t</sub>*, entropy of solid–solid transition. Standard deviations are given in parentheses. <sup>b</sup> Standard deviations less than 0.1 K are not shown.

<sup>c</sup> Δ*S<sub>m</sub>* = Δ*H<sub>m</sub>*/*T<sub>m</sub>*. <sup>d</sup> Δ*S<sub>t</sub>* = Δ*H<sub>t</sub>*/*T<sub>t</sub>*.

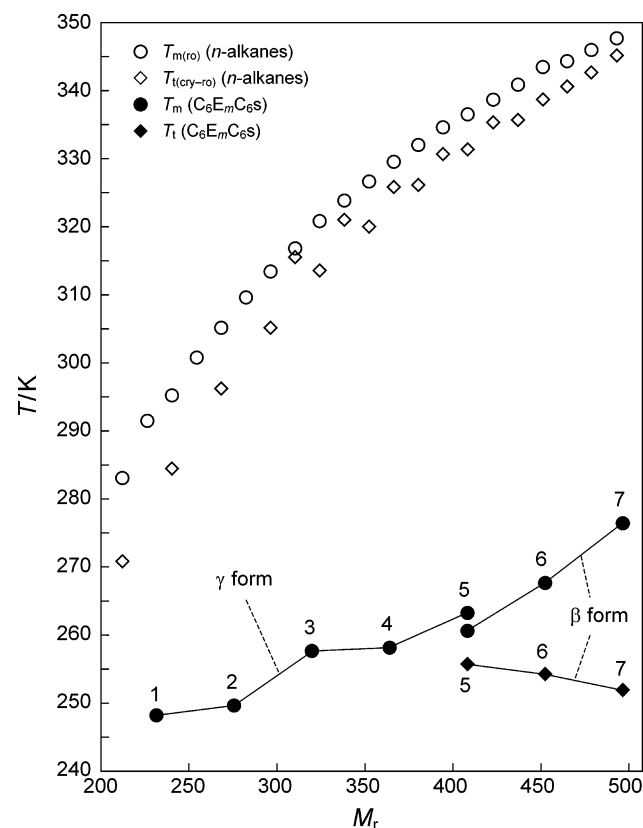


Figure 4. *T<sub>m</sub>* and *T<sub>t</sub>* for C<sub>6</sub>E<sub>m</sub>C<sub>6</sub>s, and *T<sub>m(ro)</sub>* and *T<sub>t(cry-ro)</sub>* for *n*-alkanes. The number of oxyethylene units *m* for C<sub>6</sub>E<sub>m</sub>C<sub>6</sub>s is shown by numerals.

rotator phase (Δ*H<sub>m(ro)</sub>*) and a sum (Δ*H<sub>sum</sub>*) of the enthalpy of crystalline–rotator phase transition (Δ*H<sub>t(cry-ro)</sub>*) and Δ*H<sub>m(ro)</sub>* for pertinent *n*-alkanes.<sup>21</sup> It should be noted that in our analysis we use Δ*H<sub>sum</sub>* of *n*-alkanes, rather than Δ*H<sub>m(ro)</sub>*, for comparing with Δ*H<sub>m</sub>* of C<sub>6</sub>E<sub>m</sub>C<sub>6</sub>s (γ form), because the crystalline alkanes melt via the rotator phase. The dependencies on *M<sub>r</sub>* of the entropy of melting (Δ*S<sub>m</sub>*) and the entropy of solid–solid transition (Δ*S<sub>t</sub>*) for C<sub>6</sub>E<sub>m</sub>C<sub>6</sub>s are shown in Figure 6, where, similarly to the case of the enthalpy, the dependencies of the entropy of melting of the rotator phase (Δ*S<sub>m(ro)</sub>*) and a sum (Δ*S<sub>sum</sub>*) of the entropy of crystalline–rotator phase transition (Δ*S<sub>t(cry-ro)</sub>*) and Δ*S<sub>m(ro)</sub>* for *n*-alkanes are also given.<sup>21</sup>

In what follows, we will discuss the melting behavior of the γ form solid of C<sub>6</sub>E<sub>1</sub>C<sub>6</sub>, C<sub>6</sub>E<sub>2</sub>C<sub>6</sub>, C<sub>6</sub>E<sub>3</sub>C<sub>6</sub>, C<sub>4</sub>E<sub>6</sub>C<sub>4</sub>, and C<sub>6</sub>E<sub>5</sub>C<sub>6</sub> (annealed) and of the β form solid of C<sub>6</sub>E<sub>5</sub>C<sub>6</sub> (unannealed), C<sub>6</sub>E<sub>6</sub>C<sub>6</sub>, and C<sub>6</sub>E<sub>7</sub>C<sub>6</sub>.

(a) *Melting of the γ Form Solid.* In our preliminary study,<sup>15</sup> we have compared the values of *T<sub>m</sub>*, Δ*H<sub>m</sub>*, and Δ*S<sub>m</sub>* of some γ

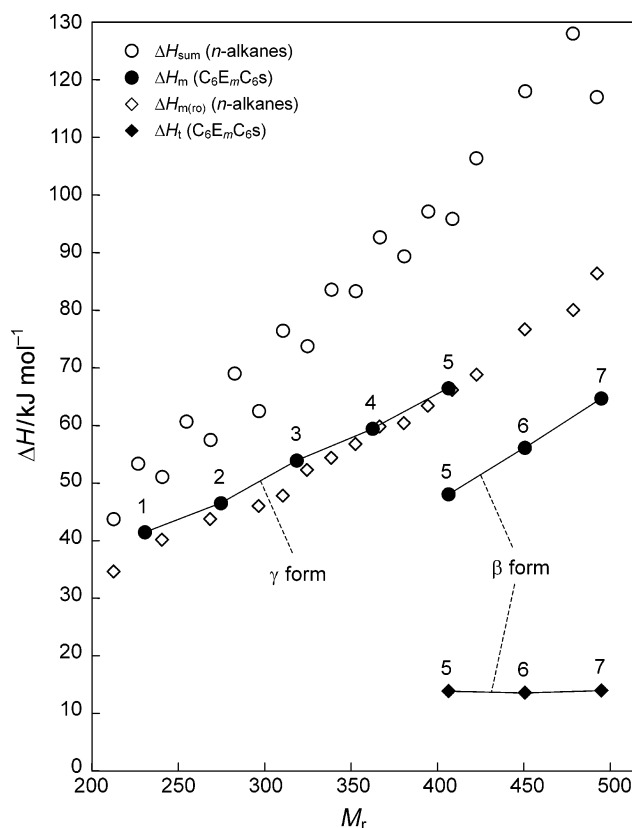
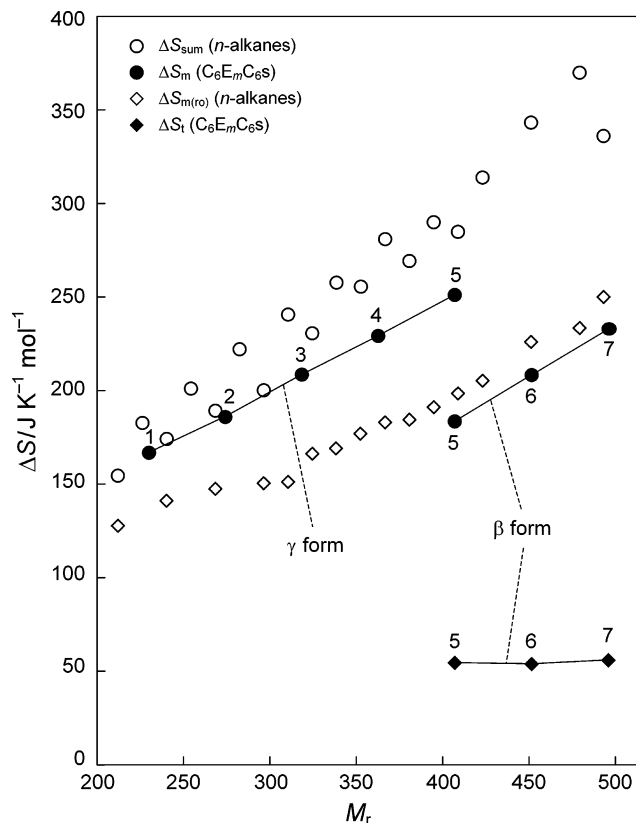


Figure 5. Δ*H<sub>m</sub>* and Δ*H<sub>t</sub>* for C<sub>6</sub>E<sub>m</sub>C<sub>6</sub>s, and Δ*H<sub>sum</sub>* and Δ*H<sub>m(ro)</sub>* for *n*-alkanes. The number of oxyethylene units *m* for C<sub>6</sub>E<sub>m</sub>C<sub>6</sub>s is shown by numerals.

form C<sub>n</sub>E<sub>m</sub>C<sub>n</sub>s with the corresponding quantities of *n*-alkanes. The more accurate thermodynamic quantities determined in this work for the purified samples of C<sub>6</sub>E<sub>m</sub>C<sub>6</sub>s allow us to examine their melting behavior more closely.

In Figure 4, two interesting features are noted. The first is the odd–even alternation of *T<sub>m</sub>* for the γ form C<sub>6</sub>E<sub>m</sub>C<sub>6</sub>s with respect to the number of oxyethylene units (*m*). This phenomenon is similar to that observed for *n*-alkanes, which has been well-established and interpreted. Because one oxyethylene unit contains three backbone atoms (one oxygen and two carbons), the parity of the number of backbone atoms in a whole molecule (*N<sub>b</sub>*) of C<sub>6</sub>E<sub>m</sub>C<sub>6</sub> alternates every one unit of *m*. The observation of the odd–even alternation of *T<sub>m</sub>* strongly suggests that crystal packing of planar C<sub>6</sub>E<sub>m</sub>C<sub>6</sub> molecules alternates depending on the parity of *N<sub>b</sub>*, similar to the case of *n*-alkane molecules.<sup>18</sup> This is the first time that the odd–even alternation of *T<sub>m</sub>* has been found for the all-trans modification of C<sub>n</sub>E<sub>m</sub>C<sub>n</sub>s.





**Figure 6.**  $\Delta S_m$  and  $\Delta S_t$  for  $C_6E_mC_6S$ , and  $\Delta S_{sum}$  and  $\Delta S_{m(ro)}$  for  $n$ -alkanes. The number of oxyethylene units  $m$  for  $C_6E_mC_6S$  is shown by numerals.

The second feature in Figure 4 is that the values of  $T_m$  for  $C_6E_mC_6S$  are much lower than the values of  $T_{m(ro)}$  for  $n$ -alkanes with similar values of  $M_r$ . Actually, the  $C_6E_mC_6$  compounds ( $m \leq 7$ ) are liquid at room temperature, in contrast to the solid for the  $n$ -alkanes except for a few shorter homologues. The big difference of the melting point between the  $\gamma$  form  $C_6E_mC_6S$  and  $n$ -alkanes, both of which have the all-trans planar structure in the solid state, is a noteworthy observation. While the values of  $T_m$  and  $T_{m(ro)}$  for  $C_6E_mC_6S$  and  $n$ -alkanes increase with increasing  $M_r$ , the rate of increase for the former is much lower than that for the latter. Thus, the difference in values of the melting point between  $C_6E_mC_6S$  and  $n$ -alkanes becomes larger with increasing  $M_r$ . We will discuss below possible factors that lower the melting point of the  $\gamma$  form  $C_6E_mC_6S$ .

Figure 5 shows that the values of  $\Delta H_m$  for  $C_6E_mC_6S$  are considerably smaller than the values of  $\Delta H_{sum}$  for the corresponding  $n$ -alkanes. For the  $\gamma$  form  $C_6E_mC_6S$  ( $m = 1-5$ ), the values of  $\Delta H_m$  separate more from the values of  $\Delta H_{sum}$  with increasing  $m$  and come closer in turn to the values of  $\Delta H_{m(ro)}$ . This observation implies that the introduction of an oxyethylene unit ( $OCH_2CH_2$ ) into the molecule reduces the increase of  $\Delta H_m$  with increasing  $M_r$  as compared with the introduction of the corresponding alkyl unit ( $CH_2CH_2CH_2$ ). At  $m = 5$  where the polymorphism is exhibited, the value of  $\Delta H_m$  coincides substantially with the value of  $\Delta H_{m(ro)}$  for the corresponding  $n$ -alkane.

The reduction of the increase of  $\Delta H_m$  for the  $\gamma$  form  $C_6E_mC_6S$  with increasing  $M_r$ , as mentioned above, can be explained by several possible factors such as a conformational restoring force resulting from a tendency of the oligo(oxyethylene) chain to resume its intrinsic helical structure, intermolecular local dipole-dipole interactions of the polar C—O bonds, and the presence of a small void between the planar oligo(oxyethylene)

chains in the crystal.<sup>12</sup> The conformational restoring force in the oligo(oxyethylene) block opposes the intermolecular packing force in the alkyl blocks, leading to an increase of the Gibbs energy of crystal for  $C_6E_mC_6S$  relative to that for  $n$ -alkanes and resulting in a reduction of the increase of  $\Delta H_m$  with increasing  $M_r$ . The increase of the Gibbs energy of crystal in the event accounts for the lowered values of  $T_m$  for  $C_6E_mC_6S$ . The intermolecular local dipole-dipole interaction acts either as attraction or as repulsion. As the melting points for dialkyl ethers are lower than those for the corresponding  $n$ -alkanes, e.g., 230.8 K for di- $n$ -hexyl ether ( $(n-C_6H_{13})_2O$ ) compared to 267.8 K for  $n$ -tridecane ( $n-C_{13}H_{28}$ ), this interaction is also an important factor lowering the melting point of  $C_6E_mC_6S$ . The small void between the planar oligo(oxyethylene) chains, arising from the geometrical consequence that the cross-sectional area of the oligo(oxyethylene) chain ( $0.172 \text{ nm}^2$ ) is smaller than that of the alkyl chain ( $0.183 \text{ nm}^2$ ), is regarded as a defect in crystal. This factor thus increases the Gibbs energy of crystal.

As noted above, the values of  $\Delta H_m$  for the  $\gamma$  form  $C_6E_mC_6S$  become closer to the values of  $\Delta H_{m(ro)}$  for  $n$ -alkanes with increasing  $m$ . This behavior of  $\Delta H_m$  results primarily from an increasing contribution of the conformational restoring force in the oligo(oxyethylene) block in the crystal, and a conformational transformation from the planar  $\gamma$  form to the planar/helical/planar triblock  $\beta$  form eventually takes place at  $m = 5$ , where the value of  $\Delta H_m$  coincides with the value of  $\Delta H_{m(ro)}$  for the corresponding  $n$ -alkane. This result shows that the planar structure of the oligo(oxyethylene) chain is stabilized by the force of the magnitude that maintains the rotator phase of  $n$ -alkanes.

According to the results in Figure 6, the values of  $\Delta S_m$  for the  $\gamma$  form  $C_6E_mC_6S$  are slightly smaller than the values of  $\Delta S_{sum}$  for the corresponding  $n$ -alkanes. The values of  $\Delta S_m$  increase with increasing  $M_r$  less rapidly than the values of  $\Delta S_{sum}$  for  $n$ -alkanes. This result implies that the introduction of an oxyethylene unit into the molecule reduces the increase of  $\Delta S_m$  with increasing  $M_r$  as compared with the introduction of the corresponding alkyl unit.

We now elucidate the observed behavior of the entropy of melting for the  $\gamma$  form  $C_6E_mC_6S$  in comparison with the entropy for  $n$ -alkanes. For flexible linear molecules, the entropy of melting  $\Delta S_m$  can be expressed as a sum of three terms,  $\Delta S_v$ ,  $\Delta S_d$ , and  $\Delta S_c$ , where  $\Delta S_v$  is a change in entropy due to the increase in volume on melting,  $\Delta S_d$  is a change in entropy due to the occurrence of long-range disorder including the changes of the position and the orientation of molecules, and  $\Delta S_c$  is a change in entropy due to the increased conformational freedom of molecules in the melt.<sup>22-25</sup> Since the magnitudes of  $\Delta S_v$  for  $C_6E_mC_6S$  and  $n$ -alkanes are most probably not appreciably different from one another, we will consider only the two terms,  $\Delta S_d$  and  $\Delta S_c$ .

The entropy change  $\Delta S_d$  is related to the randomness of molecular configurations in the melt. As the local miscibility of the oligo(oxyethylene) and alkyl blocks is low, they tend to separate from one another, resulting in the formation of their domains in the melt with structural organization, like the microdomain structure of block copolymers.<sup>26</sup> Accordingly, the increase of the fraction of the oligo(oxyethylene) block in the  $C_6E_mC_6$  molecule should promote the formation of organized structure in the melt and should give rise to a decrease of  $\Delta S_d$ , which then contributes to lowering  $\Delta S_m$ . The term  $\Delta S_c$ , on the other hand, is related to the flexibility of the molecule. As oligo(oxyethylene) chains are more flexible than  $n$ -alkyl chains,<sup>27</sup> the increase of the fraction of the oligo(oxyethylene) block in

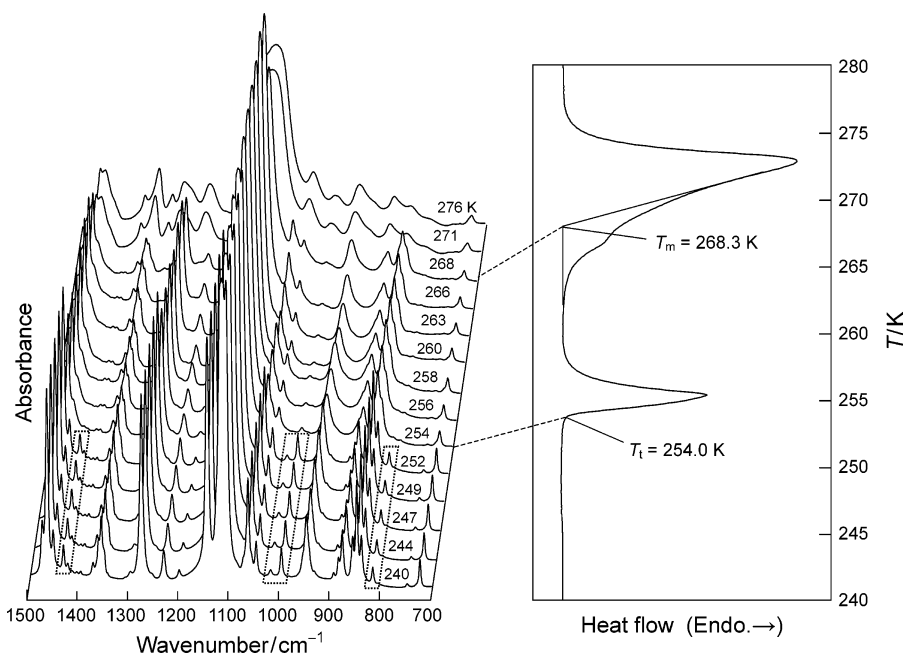


**Figure 7.** Infrared spectra at various temperatures and a DSC melting curve of  $C_6E_6C_6$ .

the  $C_6E_mC_6$  molecule leads to an increase of  $\Delta S_c$ . This term then contributes to raising  $\Delta S_m$ .

As noted in Figure 6, the rate of increase in  $\Delta S_m$  for the  $\gamma$  form  $C_6E_mC_6$ s with increasing  $M_r$  is lower than that in  $\Delta S_{sum}$  for  $n$ -alkanes. This observed behavior of  $\Delta S_m$  can be attributed to  $\Delta S_d$ , because this term decreases with the introduction of oxyethylene units in the molecule. It is shown therefore that  $\Delta S_d$  contributes, to a greater extent, to  $\Delta S_m$  of  $C_6E_mC_6$ s than  $\Delta S_c$ .

The entropy of mixing of the oligo(oxyethylene) and alkyl blocks in the melt can be a possible factor in accounting in part for the melting behavior of  $C_6E_mC_6$ s. No substantial differences in the observed entropy of melting between  $C_6E_mC_6$ s and  $n$ -alkanes (Figure 6) may suggest this factor not to be significant. We refrain from further discussion because of the uncertain state of the mixing for the  $C_6E_mC_6$  compounds studied.

**(b) Melting of the  $\beta$  Form Solid.** The DSC melting curves of  $C_6E_5C_6$  (unannealed),  $C_6E_6C_6$ , and  $C_6E_7C_6$  show two main endotherms (Figure 2), indicating the presence of a solid–solid transition. To study the structural changes that occur at this transition, we have examined the changes of the infrared spectra with temperature. The spectra of  $C_6E_6C_6$ , as an example, measured at various temperatures are shown in Figure 7, along with the relevant DSC melting curve measured at a rate of heating of  $3.0 \text{ deg min}^{-1}$ . The spectral features distinctly change between 252 and 254 K and between 268 and 271 K. The temperatures at which these spectral changes occur coincide with  $T_i$  (254.0 K) and  $T_m$  (268.3 K), respectively, determined by the DSC measurement. At temperatures below  $T_i$ , the  $C_6E_6C_6$  molecule assumes the  $\beta$  form with the planar structure in the end alkyl blocks and the helical structure in the central oligo(oxyethylene) block. With increasing temperature, the infrared bands at 817, 1000, 1021, and  $1435 \text{ cm}^{-1}$ , shown boxed off in Figure 7, assigned to the alkyl chains of the  $\beta$  form disappear at 254 K, and no bands assignable to the ordered structure of the alkyl blocks are observed above this temperature. These observations show that, above the solid–solid transition temperature  $T_i$ , the alkyl blocks in the  $C_6E_6C_6$  molecule are disordered or almost melted. The bands associated with the oligo(oxyethylene) block (e.g., those at 848, 1115, and  $1280$

$\text{cm}^{-1}$ ), on the other hand, remain substantially unchanged through this transition. It is shown therefore that the  $C_6E_6C_6$  crystal has a partially melted structure in a temperature range between  $T_i$  and  $T_m$  (254.0–268.3 K). Similar spectral observations have been made for other  $\beta$  form  $C_6E_mC_6$ s.

Figure 4 shows the contrasting dependencies of  $T_i$  and  $T_m$  for the  $\beta$  form  $C_6E_mC_6$ s on the number of oxyethylene units ( $m$ ). This result is obviously correlated with the fact that the phase transitions are accompanied by structural changes in the respective blocks as described above. We now examine the observed behavior of the enthalpy of solid–solid transition  $\Delta H_i$  for  $C_6E_mC_6$ s with respect to the structural changes of the alkyl blocks. To do this, we compare the observed values of  $\Delta H_i$  with the values of the enthalpy of melting for perfectly crystalline polyethylene ( $\Delta H_m(\text{PE})$ ) and for the rotator phase of polyethylene ( $\Delta H_{m(\text{ro})}(\text{PE})$ ). The values for  $\Delta H_m(\text{PE})$  and  $\Delta H_{m(\text{ro})}(\text{PE})$  at a melting point  $T_m$  can be evaluated by using the equations<sup>28,29</sup>

$$\Delta H_m(\text{PE}) = -2.33 + (3.04 \times 10^{-2})T_m - (3.72 \times 10^{-5})T_m^2$$

and

$$\Delta H_{m(\text{ro})}(\text{PE}) = -5.24 + (2.67 \times 10^{-4})T_m + (2.38 \times 10^{-4})T_m^2 - (4.93 \times 10^{-7})T_m^3$$

where  $T_m$  is given in units of K, and  $\Delta H_m(\text{PE})$  and  $\Delta H_{m(\text{ro})}(\text{PE})$  are given in units of  $\text{kJ (mol of } \text{CH}_2)^{-1}$ . Assuming that the alkyl  $\text{CH}_3(\text{CH}_2)_5$  blocks in the  $C_6E_mC_6$  molecule are perfectly crystalline, we obtain using the above equation for  $\Delta H_m(\text{PE})$  the values for  $\Delta H_i$  (melting of the alkyl blocks) as 36.10, 35.87, and  $35.51 \text{ kJ mol}^{-1}$  for  $C_6E_5C_6$  (unannealed),  $C_6E_6C_6$ , and  $C_6E_7C_6$ , respectively. The corresponding observed values are 13.91, 13.61, and  $14.00 \text{ kJ mol}^{-1}$  (Table 2), which are about 40% the calculated values for  $\Delta H_i$ . Assuming, on the other hand, that the  $\text{CH}_3(\text{CH}_2)_5$  blocks are packed in the crystal in the same fashion as the rotator phase of polyethylene, we obtain using the equation for  $\Delta H_{m(\text{ro})}(\text{PE})$  the values for  $\Delta H_i$  as 25.68, 25.20, and  $24.50 \text{ kJ mol}^{-1}$  for  $C_6E_5C_6$  (unannealed),  $C_6E_6C_6$ , and  $C_6E_7C_6$ , respectively. The observed values are about 55% the

calculated values for  $\Delta H_t$ . The results that the observed values of  $\Delta H_t$  are considerably smaller than the values for crystalline polyethylene and rotator-phase polyethylene suggest that the alkyl chains in the  $\beta$  form  $C_6E_mC_6$ s are loosely packed in the crystal even below  $T_t$ . This can be explained by the structural adaptation of the alkyl chain to a void with a surplus capacity allowed by the bulky helical structure of the oligo(oxyethylene) block.<sup>12</sup> The observed small values of  $\Delta H_t$  can also be ascribed in part to the peculiar structure of the  $\beta$  form; namely, the alkyl  $CH_2CH_2CH_2(O)$  groups adjoining the central oligo(oxyethylene) block are involved in the helical structure inherent in the oligo(oxyethylene) chain (Figure 1), and the all-trans structure of the alkyl chain is shortened accordingly.

We next discuss the observed behavior of the enthalpy of melting  $\Delta H_m$  for  $C_6E_mC_6$ s. As the alkyl blocks are substantially melted above the solid–solid transition temperature  $T_t$ , the enthalpy of melting  $\Delta H_m$  is associated almost exclusively with the melting of the helical oligo(oxyethylene) block in the molecule. Thus, similarly to the case of  $\Delta H_t$ , we can compare the observed values of  $\Delta H_m$  with the value of the enthalpy of melting for perfectly crystalline poly(oxyethylene) ( $\Delta H_m(\text{POE})$ ) evaluated by using the equation<sup>29</sup>

$$\Delta H_m(\text{POE}) = -8.418 + (8.94 \times 10^{-2})T_m - (1.113 \times 10^{-4})T_m^2$$

where  $\Delta H_m(\text{POE})$  is given in units of kJ (mol of  $OCH_2CH_2$ )<sup>-1</sup>. Assuming that the oligo(oxyethylene) block in the  $C_6E_mC_6$  molecule is perfectly crystalline, we obtain the values for  $\Delta H_m$  (melting of the oligo(oxyethylene) block) as 36.56, 45.34, and 54.48 kJ mol<sup>-1</sup> for  $C_6E_5C_6$  (unannealed),  $C_6E_6C_6$ , and  $C_6E_7C_6$ , respectively. The corresponding observed values are 47.86, 55.97, and 64.46 kJ mol<sup>-1</sup> (Table 2), which are approximately 20–30% larger than the calculated values for  $\Delta H_m$ . These apparently excess values of the enthalpy of melting can be explained by the peculiar structure of the  $\beta$  form as described above. The elongated helical structure, as a result of the involvement of the alkyl  $CH_2CH_2CH_2(O)$  groups, is responsible for the larger values of  $\Delta H_m$  than the values expected for the nominal oligo(oxyethylene) block.

The changes in entropy at the phase transitions provide further structural information. The values of the entropy of solid–solid transition  $\Delta S_t$ , 54.5, 53.6, and 55.7 J K<sup>-1</sup> mol<sup>-1</sup> for  $C_6E_5C_6$  (unannealed),  $C_6E_6C_6$ , and  $C_6E_7C_6$ , respectively, are much the same as one another irrespective of the number of oxyethylene units ( $m$ ). This confirms that the observed solid–solid transition is associated only with the alkyl blocks. The values of ca. 55 J K<sup>-1</sup> mol<sup>-1</sup> for the melting of the two  $CH_3(CH_2)_5$  groups in the molecule can be converted to 4.6 J K<sup>-1</sup> (mol of  $CH_2$  or  $CH_3$ )<sup>-1</sup>. This value is larger than 2–4 J K<sup>-1</sup> (mol of  $CH_2$ )<sup>-1</sup> for the crystalline–rotator phase transition of  $n$ -alkanes.<sup>18</sup> It is shown therefore that the alkyl chain is more disordered in the partially melt phase of  $C_6E_mC_6$ s than in the rotator phase of  $n$ -alkanes.

The entropy of melting  $\Delta S_m$  for the  $\beta$  form  $C_6E_mC_6$ s increases with increasing  $m$  (Figure 6). Its increment with an increase of one unit of  $m$ , which corresponds to the entropy of melting for an oxyethylene unit, is 24.7 J K<sup>-1</sup> mol<sup>-1</sup> from  $m = 5$  to 6 and is 24.8 J K<sup>-1</sup> mol<sup>-1</sup> from  $m = 6$  to 7. These values almost coincide with 24.4 J K<sup>-1</sup> (mol of  $OCH_2CH_2$ )<sup>-1</sup> for perfectly crystalline poly(oxyethylene).<sup>30</sup> This result indicates that the crystallinity of the oligo(oxyethylene) block in the  $\beta$  form solid is significantly high.

**Other Systems Involving Planar Oligo- or Poly(oxyethylene) Chains.** In addition to the  $C_nE_mC_{n'}$  triblock compounds

studied here, the all-trans planar structure of oligo- or poly(oxyethylene) chains has been found in several molecular systems. It is interesting to note that the planar structure is stabilized by various different factors. For the poly(oxyethylene) specimens stretched about 2-fold after necking, an external mechanical force is responsible for the formation of the planar structure.<sup>14</sup> The trans conformation of the  $OCH_2-CH_2O$  bonds in poly(ethylene glycol) included in a cavity of  $\alpha$ -cyclodextrin results from a hydrophobic atmosphere and an appropriate size of the host cavity.<sup>31</sup> The planar oligo(oxyethylene) structure in diblock compounds  $H(CH_2)_n(OCH_2CH_2)_mOH$  in the solid state is stabilized by an intermolecular packing force in the adjoining alkyl block,<sup>32–36</sup> as in the case of the  $C_nE_mC_{n'}$  triblock compounds.

While the planar structure of oligo- or poly(oxyethylene) chains is attained by a number of different methods, the stabilization of the planar structure in the block compounds is unique in that the stabilization arises directly from chemical bonding with alkyl or other pertinent chemical groups. This chemical stabilization of the planar structure should have possibilities of designing molecular assemblies with particular higher order structures.

**Oligo(oxyethylene) Block as a Potent Factor Governing the Formation of Higher Order Structures.** We have shown in this work that the molecular form of the block compounds consisting of the oligo(oxyethylene) chain and the alkyl chain is determined substantially by the balance of the intramolecular conformational restoring force in the oligo(oxyethylene) block and the intermolecular packing force in the alkyl block. Thus, the introduction of the oligo(oxyethylene) block into the alkyl chain weakens the effective lateral cohesive force of the alkyl chain and can therefore be a potent factor that governs the formation of higher order structures of molecular assemblies such as micelles, monolayers, Langmuir–Blodgett films, liquid crystals, and liposomes.

The control of intermolecular cohesive forces can also be achieved by other methods such as the introduction of unsaturated bonds or side chains into the alkyl chain and the mixing of homologous compounds with different chain lengths. Since the introduction of the oligo(oxyethylene) block does not significantly perturb the original geometrical structure of the molecule, this is an exquisite method for controlling the effective cohesive force of the alkyl chain.

## Conclusions

The present study has revealed the relation between the chain-length-dependent conformational transformation and melting behavior of the  $C_6E_mC_6$  triblock compounds ( $m = 1-7$ ). The compounds with  $m \leq 5$  assume the all-trans planar form ( $\gamma$  form), while those with  $m \geq 5$  assume the planar/helical/planar triblock form ( $\beta$  form). The melting points of the  $\gamma$  form  $C_6E_mC_6$ s are much lower than the melting points of  $n$ -alkanes with similar molecular mass. This result is interpreted as due to the higher Gibbs energy of crystal for  $C_6E_mC_6$ s. The  $\beta$  form  $C_6E_mC_6$ s melt stepwise through a solid–solid transition, at which the melting of only the alkyl blocks of the molecule occurs.

The molecular form of the alkyl/oligo(oxyethylene)/alkyl triblock compounds in the solid state is determined by the balance of the intramolecular conformational restoring force in the central oligo(oxyethylene) block and the intermolecular packing force in the end alkyl blocks. The introduction of the oligo(oxyethylene) block into the alkyl chain weakens the effective lateral cohesive force of the alkyl chain and can therefore be a potent factor that governs the formation of higher order structures of molecular assemblies.

**Acknowledgment.** This work was partially supported by Grants-in-Aid for Scientific Research Nos. 10640492 and 13640513 from the Ministry of Education, Culture, Sports, Science, and Technology of Japan. We thank Mr. Kenji Hashiwata and Ms. Miyuki Akisue-Okuda for their assistance in the experimental work.

## References and Notes

- (1) Séguéla, R.; Prud'homme, J. *Polymer* **1989**, *30*, 1446.
- (2) Cohen, R. E.; Cheng, P.-L.; Douzinas, K.; Kofinas, P.; Berney, C. V. *Macromolecules* **1990**, *23*, 324.
- (3) Douzinas, K. C.; Cohen, R. E.; Halasa, A. F. *Macromolecules* **1991**, *24*, 4457.
- (4) Nojima, S.; Kato, K.; Yamamoto, S.; Ashida, T. *Macromolecules* **1992**, *25*, 2237.
- (5) Domszy, R. C.; Booth, C. *Makromol. Chem.* **1982**, *183*, 1051.
- (6) Teo, H. H.; Swales, T. G. E.; Domszy, R. C.; Heatley, F.; Booth, C. *Makromol. Chem.* **1983**, *184*, 861.
- (7) Matsuura, H.; Fukuhara, K.; Hiraoka, O. *J. Mol. Struct.* **1988**, *189*, 249.
- (8) Fukuhara, K.; Sagawa, T.; Kihara, S.; Matsuura, H. *J. Mol. Struct.* **1996**, *379*, 197.
- (9) Fukuhara, K.; Sakogawa, F.; Matsuura, H. *J. Mol. Struct.* **1997**, *405*, 123.
- (10) Fukuhara, K.; Masatoki, S.; Yonemitsu, T.; Matsuura, H. *J. Mol. Struct.* **1998**, *444*, 69.
- (11) Chen, Y.; Baker, G. L.; Ding, Y.; Rabolt, J. F. *J. Am. Chem. Soc.* **1999**, *121*, 6962.
- (12) Fukuhara, K.; Hashiwata, K.; Takayama, K.; Matsuura, H. *J. Mol. Struct.* **2000**, *523*, 269.
- (13) Tadokoro, H. *Structure of Crystalline Polymers*; Wiley: New York, 1979.
- (14) Takahashi, Y.; Sumita, I.; Tadokoro, H. *J. Polym. Sci., Polym. Phys. Ed.* **1973**, *11*, 2113.
- (15) Fukuhara, K.; Akisue, M.; Matsuura, H. *Chem. Lett.* **2001**, 828.
- (16) Gibson, T. J. *Org. Chem.* **1980**, *45*, 1095.
- (17) Matsuura, H.; Fukuhara, K. *J. Polym. Sci., Part B, Polym. Phys.* **1986**, *24*, 1383.
- (18) Broadhurst, M. G. *J. Res. Natl. Bur. Stand., Sect. A* **1962**, *66*, 241.
- (19) Claudy, P.; Letoffe, J. M. *Calorim. Anal. Therm.* **1991**, *22*, 281.
- (20) Barbillon, P.; Schuffenecker, L.; Dellacherie, J.; Balesdent, D.; Dirand, M. *J. Chim. Phys. Phys.-Chim. Biol.* **1991**, *88*, 91.
- (21) Although *n*-C<sub>16</sub>H<sub>34</sub> (*M*<sub>r</sub> 226), *n*-C<sub>18</sub>H<sub>38</sub> (254), and *n*-C<sub>20</sub>H<sub>42</sub> (282) do not experience the rotator phase before melting unlike other *n*-alkanes cited in Figures 4–6, we still use for the sake of convenience the notation of *T*<sub>m(ro)</sub>,  $\Delta H_{m(ro)}$ , and  $\Delta S_{m(ro)}$  to mean their melting point, enthalpy of melting, and entropy of melting, respectively. For these compounds,  $\Delta H_{l(cry-ro)}$  and  $\Delta S_{l(cry-ro)}$  are not relevant.
- (22) Starkweather, H. W., Jr.; Boyd, R. H. *J. Phys. Chem.* **1960**, *64*, 410.
- (23) Bondi, A. *Chem. Rev.* **1967**, *67*, 565.
- (24) Turturro, A.; Bianchi, U. *J. Chem. Phys.* **1975**, *62*, 1668.
- (25) Yalkowsky, S. H. *Ind. Eng. Chem., Fundam.* **1979**, *18*, 108.
- (26) Molau, G. E. In *Block Polymers*; Aggarwal, S. L., Ed.; Plenum: New York, 1970; pp 79–106.
- (27) Flory, P. J. *Statistical Mechanics of Chain Molecules*; Hanser: Munich, Germany, 1989.
- (28) Wunderlich, B.; Dole, M. *J. Polym. Sci.* **1957**, *24*, 201.
- (29) Campbell, C.; Viras, K.; Richardson, M. J.; Masters, A. J.; Booth, C. *Makromol. Chem.* **1993**, *194*, 799.
- (30) Mandelkern, L. *J. Appl. Phys.* **1955**, *26*, 443.
- (31) Harada, A.; Li, J.; Kamachi, M. *Macromolecules* **1993**, *26*, 5698.
- (32) Matsuura, H.; Fukuhara, K. *J. Phys. Chem.* **1986**, *90*, 3057.
- (33) Fukuhara, K.; Matsuura, H. *Chem. Lett.* **1987**, 1549.
- (34) Matsuura, H.; Fukuhara, K. *J. Phys. Chem.* **1987**, *91*, 6139.
- (35) Matsuura, H.; Fukuhara, K.; Masatoki, S.; Sakakibara, M. *J. Am. Chem. Soc.* **1991**, *113*, 1193.
- (36) Fukuhara, K.; Shoden, M.; Matsuura, H. *Chem. Lett.* **2000**, 1322.